Observation of Axisymmetric Solitary Waves on the Surface of a Ferrofluid

E. Bourdin, J.-C. Bacri, and E. Falcon*

*Laboratoire Matière et Systèmes Complexes (MSC), Université Paris Diderot, CNRS (UMR 7057),
10 rue A. Domon and L. Duquet, 75 013 Paris, France*

We report the first observation of axisymmetric solitary waves on the surface of a cylindrical magnetic fluid layer surrounding a current-carrying metallic tube. According to the ratio between the magnetic and capillary forces, both elevation and depression solitary waves are observed with profiles in good agreement with theoretical predictions based on the magnetic analogue of the Korteweg–de Vries equation. We also report the first measurements of the velocity and the dispersion relation of axisymmetric linear waves propagating on the cylindrical ferrofluid layer that are found in good agreement with theoretical predictions.

PACS numbers: 47.35.Fg, 47.65.Cb

Solitary waves or solitons are localized nonlinear waves that propagate almost without deformation due to the balance between the nonlinearity and the dispersion. Since the first observation of a solitary wave on the free surface of water by Russell [1], and its interpretation using the Korteweg–de Vries equation (KdV) [2], it has been shown that the KdV equation describes a large class of solitons observed in various situations: acoustic waves on a crystal lattice, plasma waves, hydrodynamics internal or surface waves, elastic surface waves, and waves in optical fibers [3]. Most of them involve a localized elevation disturbance propagating within a quasi-one-dimensional plane system. Observations of axisymmetric solitary waves governed by the KdV equation are scarce [4], and mainly concern waves in rotating fluids confined in a tube or on vortex lines. More recently, Bashtovoi *et al.* derived a KdV equation with an axisymmetric solitary wave solution propagating on the surface of a cylindrical magnetic fluid layer submitted to a magnetic field [5,6]. Without gravity, the stability of the cylindrical magnetic fluid layer is governed by the ratio between the magnetic force and the capillary one. According to its ratio, axisymmetric elevation (humplike) or depression (holelike) solitary waves are predicted with a subsonic or supersonic velocity [5,6]. To our knowledge, direct observation of axisymmetric magnetic solitary waves has never been reported.

In this Letter, we report the first observation of axisymmetric solitary waves on the surface of a cylindrical ferrofluid layer submitted to an azimuthal magnetic field. Depending on the strength of the field, elevation or depression solitary waves are observed on the ferrofluid surface. A ferrofluid is a stable suspension of nanometric magnetic particles diluted in a carrier liquid (water or oil) that responds to an external applied magnetic field [7,8]. Although the solitary waves are damped by viscous dissipation, we have shown that they keep the self-similar profile given by the solution of the KdV equation on a propagation length larger than their typical scale.

Moreover, we also report the first measurement of the velocity and dispersion relation of axisymmetric magnetic linear waves in this system in good agreement with the theoretical predictions [9].

The experimental setup is shown in Fig. 1. It consists of a cylindrical copper tube (50 cm in length, $a = 1.5$ mm in outer radius, and 0.5 mm in thickness) placed in the middle of a rectangular Plexiglas container (40×40 mm^2 side and 30 cm length) crossing both container end sides in the center through hollow waterproof screws. A dc electrical current I in the range 0–100 A is applied to the cylindrical conductor by means of a power supply. The current generates circular magnetic field lines around the tube with a radial decreasing amplitude. The corresponding radial magnetic force stabilizes a ferrofluid layer of outer radius $2.9 \leq R \leq 5$ mm, around the tube. For the results reported below, $R = 3.8$ mm for linear waves and $R = 3.3$ mm for solitary waves. The ferrofluid used is an ionic aqueous suspension synthesized with 12.4% by volume of maghemite particles (Fe$_2$O$_3$, 7 ± 0.3 nm in diameter) [10]. The properties of this magnetic fluid are density, $\rho = 1534 \pm 1$ kg/m^3, initial magnetic susceptibility, $\chi_i = 0.75$, magnetic saturation $M_{\text{sat}} = 36 \times 10^3$ A/m, and estimated dynamic viscosity 1.4×10^{-3} N s/m^2. To avoid gravitational effects, the whole container is filled with Freon (C$_2$Cl$_3$F$_3$), a nonmiscible transparent fluid with a density, $\rho_e = 1581 \pm 1$ kg/m^3, close to the ferrofluid one. The surface tension between the ferrofluid and Freon is $\gamma = 5.5 \times 10^{-3}$ N/m. A water cooling inside the tube
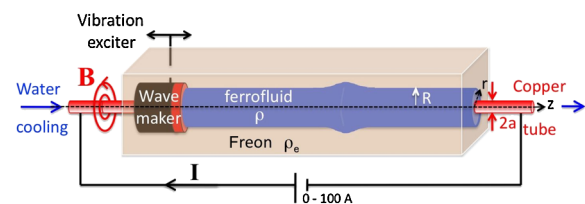

FIG. 1 (color online).   Experimental setup.

drains off the Joule dissipation of the current-carrying electrodes (their contact resistance being 13.8 mΩ, that is a dissipated power of roughly 140 W for $I = 100$ A). The metallic tube is tightened to avoid parasitic vibration. Namely, one end of the tube is threaded to fix it with a nut, and a small chuck is used at the other end to tighten it. Surface waves are generated on the ferrofluid surface by the horizontal motion of a concentrical Plexiglas tube, 9 mm (3 mm) in outer (inner) diameter driven by an electromagnetic vibration exciter. The wave maker is driven sinusoidally (in a frequency range from 0.5 to 10 Hz with a maximal amplitude of 2 mm) to study linear waves, or impulsively (typical duration of 0.05 s) to study solitary waves. Note that the wave maker end is made of copper in order to increase the ferrofluid wetting. Axisymmetric waves propagating on the cylindrical ferrofluid layer are visualized with a high-resolution camera (Pixelink 2208×3000 pixels) located above the container, and are recorded with a 25 Hz (44 Hz) sampling for linear (solitary) waves.

The magnetic induction generated by the carrying-current tube is up to 30 G at 100 A at a distance $r = 8$ mm from the tube axis, that is the z axis of the (r, θ, z) cylindrical coordinate system. The magnetic induction being orthoradial $\vec{B} \equiv [B_r = 0, B_\theta \equiv B, B_z = 0]$, i.e., throughout tangential to the free surface, the Rosensweig magnetic surface instability is absent [7,11]. B is measured with a transverse Hall probe via a Gauss meter (Bell 5100) as a function of the current and the distance r from the tube in agreement with the usual law $B = \mu_0 I/(2\pi r)$ for $r \geq a$, where $\mu_0 = 4\pi \times 10^{-7}$ H/m is the magnetic permeability of the vacuum. The corresponding magnetic body force, $\vec{F}_{\mathrm{mag}} = -\mu_0 \chi I^2/(4\pi^2 r^3)\vec{e}_r$, is radial towards the z axis. Since gravity is negligible ($\rho_e \simeq \rho$), this magnetic force stabilizes a uniform axisymmetric layer of a magnetic fluid of outer radius R as soon as the capillary force by volume $F_{\mathrm{cap}} \sim \gamma/R^2$ is small enough. Both magnetic and capillary effects are then compared by the dimensionless magnetic Bond number $\mathrm{Bo}_m \equiv F_{\mathrm{mag}}/F_{\mathrm{cap}} = \mu_0 \chi I^2/(4\pi^2 \gamma R)$.

Assuming no gravity and a thin tube radius ($a \ll R$), the dispersion relation of inviscid axisymmetric linear waves propagating on a magnetic fluid surface reads [9,11]

$$\omega^2 = \frac{\gamma}{\rho R^3} kR[\mathrm{Bo}_m - 1 + (kR)^2]\frac{I_1(kR)}{I_0(kR)}, \qquad (1)$$

where $\omega \equiv 2\pi f$ is the angular frequency and $k \equiv 2\pi/\lambda$ the wave number, I_n and K_n being, respectively, the modified Bessel functions of first and second kind of order n (their ratio being a positive increasing function of k). When $\mathrm{Bo}_m \leq 1$, the capillary effects are greater than the magnetic ones, and an instability occurs [$\omega^2 \leq 0$ in Eq. (1)]: the cylindrical ferrofluid layer is unstable to disturbances whose wavelengths $\lambda \geq 2\pi R/\sqrt{\mathrm{Bo}_m - 1}$, and breaks up into a string of connected drops [9,12]. This is the magnetic analogue of the surface-tension-driven Rayleigh-Plateau

instability when a thin cylindrical jet of a usual fluid breaks into a set of drops [13]. When $\mathrm{Bo}_m > 1$, one has $\omega^2 > 0$ in Eq. (1): the cylindrical layer of ferrofluid is stable whatever the wavelength disturbance, and axisymmetric linear waves can propagate on its surface.

We first measure the dispersion relation of such linear waves. The wave maker is driven sinusoidally in order to generate surface waves at the interface between the Freon and the ferrofluid. A typical snapshot of such axisymmetric linear waves is shown in the bottom inset of Fig. 2. The top inset of Fig. 2 shows the wavelength λ of surface waves in response to the forcing frequency f for different applied currents I, that is, for different $\mathrm{Bo}_m \sim I^2$ ranging from 1 to 12. λ is found to decrease with increasing frequency whatever Bo_m. When expressed in the rescaled variables $\omega^2/\{[\mathrm{Bo}_m - 1 + (kR)^2]\gamma/(\rho R^3)\}$ and kR, all these data collapse on one single master curve (solid line) predicted by Eq. (1) (see Fig. 2). Note that no adjustable parameter is used when comparing the data and the theoretical dispersion relation of axisymmetric magnetic surface waves.

Using the expansion of the modified Bessel functions $\frac{I_1(x)}{I_0(x)} \sim \frac{x}{2} - \frac{x^3}{16}$ [14], the dispersion relation of Eq. (1) in a long-wavelength limit ($kR \ll 1$) reads [6]

$$\omega = c_0 k\left[1 - \frac{1}{16}\frac{\mathrm{Bo}_m - 9}{\mathrm{Bo}_m - 1}k^2 R^2\right],$$
$$c_0 = \sqrt{\frac{\gamma}{\rho R}}\sqrt{\frac{\mathrm{Bo}_m - 1}{2}}, \qquad (2)$$

where c_0 is the velocity of linear waves for $\mathrm{Bo}_m > 1$. Note
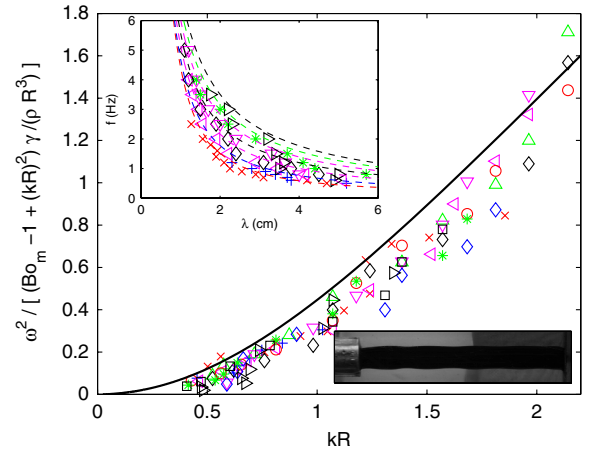

FIG. 2 (color online). Dimensionless dispersion relation of linear cylindrical waves for various applied currents I from 40 to 100 A corresponding to $\mathrm{Bo}_m = 1.85$ ($\times$), 2.69 (+), 4.17 ($\triangleleft$), 4.89 ($\triangle$), 5.67 ($\diamond$), 6.51 ($\bigcirc$), 7.4 (∇), 8.36 ($\diamond$), 9.37 (*), 10.44 ($\square$), and 11.57 ($\triangleright$). Solid line corresponds to the theoretical prediction of Eq. (1). Top inset: Frequency f as a function of the wavelength λ for different I with a 10 A step. Dashed lines are from Eq. (1). Bottom inset: Snapshot of linear waves ($f = 3.5$ Hz, $\mathrm{Bo}_m = 6.5$—wave maker is visible on the left-hand side—10 cm size window).

that both c_0 and the sign of the dispersive term $\sim k^3$ in Eq. (2) depend on Bo_m. In order to extract the velocity of linear waves, the inset of Fig. 3 displays the previous data in variables $\omega/(c_0/R)$ and kR. As expected, for small kR, all the data collapse on a single linear curve of slope 1. Note that for larger kR and for $\mathrm{Bo}_m \simeq 1$, a departure from the prediction of the linear term of Eq. (2) is observed since the dispersive effects become important [i.e., the $k^2/(\mathrm{Bo}_m - 1)$ term in Eq. (2)]. For $kR \ll 1$, the slope of each curve ω vs k thus gives, for each Bo_m value, a direct measurement of the velocity of linear waves. These values are plotted in Fig. 3 and are found in rough agreement with the theoretical velocity of Eq. (2) with no adjustable parameter. To our knowledge this is the first measurement of the velocity and dispersion relation of axisymmetric magnetic linear waves on the surface of a ferrofluid.

Let us now focus on axisymmetric magnetic solitary waves. First, let us assume no viscosity and no gravity. In the long-wavelength limit ($kR \ll 1$), the dispersion is small and the linear wave velocity is c_0. When the interface deflection $A(z, t)$ is also small, such that nonlinear effects have the same order of magnitude as dispersive ones, it is governed at the leading order by a magnetic analogue of the Korteweg–de Vries equation [5,6]

$$A_t + c_0 A_z + \alpha A A_z + \beta A_{zzz} = 0, \qquad (3)$$

with $\alpha = \frac{2\mathrm{Bo}_m - 3}{2^{3/2}\sqrt{\mathrm{Bo}_m - 1}}\sqrt{\frac{\gamma}{\rho R^3}}$ the nonlinear coefficient, $\beta = \frac{\mathrm{Bo}_m - 9}{2^{9/2}\sqrt{\mathrm{Bo}_m - 1}}\sqrt{R^3 \gamma/\rho}$ the dispersive coefficient, and $\mathrm{Bo}_m > 1$. The axisymmetric magnetic solitary wave solution of Eq. (3) reads [5,6]
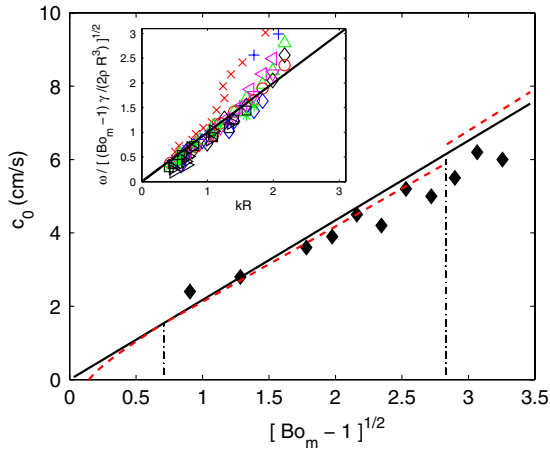

FIG. 3 (color online). Velocity of linear axisymmetric magnetic waves as a function of rescaled magnetic Bond number. Experimental (◆) and theoretical [solid line of Eq. (2)] linear wave velocity c_0. Dashed line: Theoretical solitary wave velocity c of Eq. (5) with $A_0 = 0.5$ mm, $R = 3.8$ mm (see text). Dash-dotted lines correspond to $\mathrm{Bo}_m = 3/2$ and 9. Inset: Rescaled dispersion relation $\omega/(c_0/R)$ vs kR. Same symbols as Fig. 2. Solid line has a slope 1.

$$A(z, t) = A_0 \mathrm{sech}^2\left(\frac{z - ct}{L}\right), \qquad L = \sqrt{\frac{3R^3}{2A_0}\frac{\mathrm{Bo}_m - 9}{2\mathrm{Bo}_m - 3}}, \qquad (4)$$

with c the velocity of solitary wave

$$c = c_0\left(1 + \frac{A_0}{6R}\frac{2\mathrm{Bo}_m - 3}{\mathrm{Bo}_m - 1}\right), \qquad (5)$$

and L is the length scale of the solitary wave. Equations (4) and (5) show that there exists a continuous family of soliton solutions with parameter A_0 (the extremum amplitude of the wave). Since α, β, c, and L depend on Bo_m, an elevation ($A_0 > 0$) or depression ($A_0 < 0$) solitary wave is predicted that propagates with a supersonic ($c > c_0$) or subsonic ($c < c_0$) speed. All the possible solutions are summarized in Table I.

We have performed a study of axisymmetric solitary waves on the surface of the ferrofluid layer ($R = 3.3$ mm) around a copper tube carrying current in the range 60–110 A ($4 \leq \mathrm{Bo}_m \leq 14$). We impulsively drive the shaker to generate solitary waves: the wave maker is pushed forward to generate a pulse on the fluid interface leading to either an elevation or a depression pulse according to the value of Bo_m. The interface deflection $A(z, t)$ is detected from the images recorded by the camera using standard IMAGEJ binarization and edge detection processes. The profile is displayed in Fig. 4(a) for a depression pulse ($\mathrm{Bo}_m = 8.3$) and in Fig. 4(b) for an elevation pulse ($\mathrm{Bo}_m = 10.5$). Both recordings are in good agreement with the profiles of elevation and depression KdV solitary waves given by Eq. (4). Note that once A_0 is known the theoretical profile as well as the velocity of the solitary wave given by Eqs. (4) and (5) do not involve any adjustable parameter. Those isolated pulses involve typical amplitude and size that are in the range of validity required for the derivation of Eq. (3), that is, corresponding to small dispersion ($L^2 \gg R^2$), and small nonlinearities ($|A_0| \ll R$), both of the same order of magnitude ($R^3 \sim |A_0|L^2$). Note that no solitary wave has been observed for $\mathrm{Bo}_m < 4$ since its predicted amplitude ($A_0 \sim$ few mm for $L \sim 1$ cm) is too large compared to our radius R to have small nonlinearities. The inset of Fig. 4(a) [Figure 4(b)] shows the profile of the depression (elevation) pulse recorded at different times corresponding to a total propagation distance up to 10 times its typical size. The recorded profiles are in good agreement with the KdV magnetic solitary wave all along the

TABLE I. Properties of axisymmetric solitary wave solution of Eqs. (4) and (5) according to the magnetic Bond number.

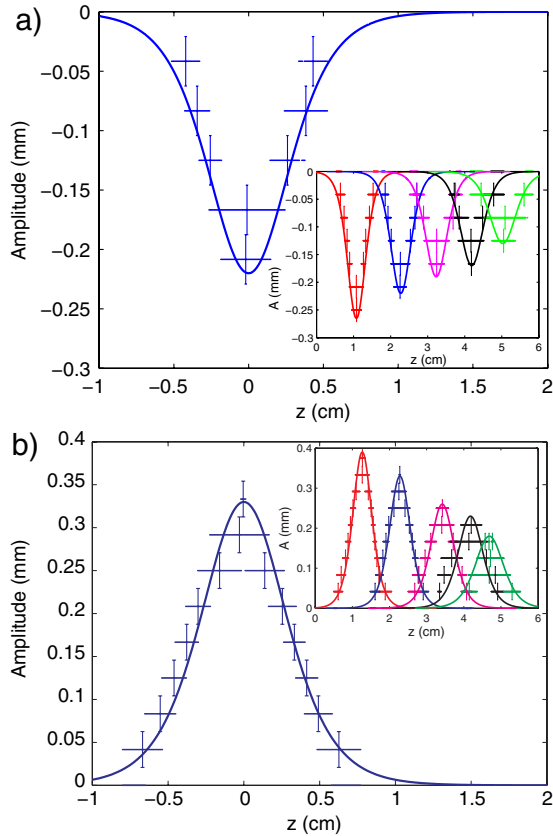| Bo_m	α	β	c	A_0	Solitary wave
$1 < \mathrm{Bo}_m < 3/2$	−	−	$<c_0$	+	Subsonic elevation
$3/2 < \mathrm{Bo}_m < 9$	+	−	$<c_0$	−	Subsonic depression
$\mathrm{Bo}_m > 9$	+	+	$>c_0$	+	Supersonic elevation

FIG. 4 (color online). (a) Axisymmetric profile of a depression magnetic solitary wave for $Bo_m = 8.3$ ($I = 80$ A), $t = 0.33$ s, (b) elevation magnetic solitary wave for $Bo_m = 10.5$($I = 90$ A), $t = 0.32$ s, centered on its extremum. Solid lines are the theoretical profiles of KdV solitons derived from Eq. (4) with no adjustable parameter. Insets: Profiles of solitary waves at different times [(a) 0.16, 0.33, 0.47, 0.62, and 0.74 s; (b) 0.17, 0.32, 0.47, 0.58, and 0.65 s] during its propagation over 10 times its typical size $L \sim 4$ mm. Initial amplitudes $A_0 = \pm 0.5$ mm. $R = 3.3$ mm. z-axis origin is located on the wave maker.

propagation. Note, however, that for farther distances the cumulative effect of dissipation leads to small amplitudes that are hardly measurable by the camera (0.04 mm/pixel). For both the elevation and depression solitary waves, dissipation leads to an extremum amplitude $A_0(z)$ that decreases linearly with the propagation distance z. By rescaling all the profiles displayed in each inset of Fig. 4 with the variables $|A(z)/A_0(z)|$ vs z/L, all the data lie on a single curve predicted by Eq. (4) (not shown here). This means that the pulse keeps a self-similar shape over a distance up to 10 times its typical size and is in a good agreement with the profile derived from KdV magnetic equation. Finally, the solitary wave velocity c is measured all along its propagation by the successive locations of amplitude extrema, $|A_0(z)|$, at different times. We find that $c \simeq c_0$ ($\sim$few cm/s) with a dependence on Bo_m

roughly comparable to that predicted by Eq. (2). Note that c is predicted by Eq. (5) to slightly depend on A_0 with a correction with respect to c_0 up to 10% when $Bo_m \sim 10$ (see dotted line in Fig. 3). Since our velocity measurement accuracy is 6%, we cannot thus discriminate from a subsonic to a supersonic solitary wave as predicted in Table I (see also Fig. 3).

In conclusion, we have reported the first observation of depression and elevation axisymmetric solitary waves on the surface of a cylindrical magnetic fluid layer and found that their shapes are in good agreement with the ones predicted from the axisymmetric KdV solitary wave solutions. A possible extension of this work would be the study of the collisions between these new solitary waves.

*Corresponding author.
eric.falcon@univ-paris-diderot.fr

[1] J. S. Russell, in *Proceedings of the Fourteenth Meeting of the British Association for the Advancement of Science, York, 1844* (John Murray, London, 1845), pp. 311–390.

[2] D. J. Korteweg and G. De Vries, Philos. Mag. **39**, 422 (1895).

[3] M. Peyrard and T. Dauxois, *Physics of Solitons* (Cambridge University Press, Cambridge, England, 2006).

[4] S. Lebovitch, J. Fluid Mech. **42**, 803 (1970); W. G. Pritchard, J. Fluid Mech. **42**, 61 (1970); T. Maxworthy, E. J. Hopfinger, and K. G. Redekopp, J. Fluid Mech. **151**, 141 (1985); P. D. Weidman and R. Zakhem, J. Fluid Mech. **191**, 557 (1988).

[5] V. G. Bashtovoi and R. A. Foigel, Magnetohydrodynamics **19**, 160 (1983); V. Bashtovoi, A. Rex, and R. Foigel, J. Magn. Magn. Mater. **39**, 115 (1983).

[6] D. Rannacher and A. Engel, New J. Phys. **8**, 108 (2006).

[7] R. E. Rosensweig, *Ferrohydrodynamics* (Dover, New York, 1997).

[8] E. Blums, A. Cebers, and M. M. Maiorov, *Magnetic Fluids* (Walter de Gruyter, Berlin,1997).

[9] V. I. Arkhipenko, Yu. D. Barkov, V. G. Bashtovoi, and M. S. Krakov, Fluid Dyn. **15**, 3 (1980).

[10] The ferrofluid synthesis has been performed by the Laboratory LI2C, University Pierre et Marie Curie–Paris 6.

[11] B. Berkovsky and V. Bashtovoi, IEEE Trans. Magn. **16**, 288 (1980).

[12] V. I. Arkhipenko and Yu. D. Barkov, J. Appl. Mech. Tech. Phys. **21**, 98 (1980).

[13] J. Plateau, Mem. Acad. R. Sci. Lett. Beaux-Arts Belg. **23**, 5 (1849); R. J. Donnelly and W. Glaberson, Proc. R. Soc. A **290**, 547 (1966).

[14] M. Abramowitz and I. Stegun, *Handbook of Mathematical Functions* (Dover, New York, 1964).